

Article

Not peer-reviewed version

Tropical Cyclonic Energy Variability in North Indian Ocean: Insights from ENSO

[Debanjana Das](#)*, [Sen Chiao](#), Chayan Roychoudhury, Fatema Khan, Sutapa Chaudhuri, Sayantika Mukherjee

Posted Date: 12 October 2023

doi: 10.20944/preprints202310.0749.v1

Keywords: tropical cyclone; ENSO; ACE; SST; SSH



Preprints.org is a free multidiscipline platform providing preprint service that is dedicated to making early versions of research outputs permanently available and citable. Preprints posted at Preprints.org appear in Web of Science, Crossref, Google Scholar, Scilit, Europe PMC.

Copyright: This is an open access article distributed under the Creative Commons Attribution License which permits unrestricted use, distribution, and reproduction in any medium, provided the original work is properly cited.

Article

Tropical Cyclonic Energy Variability in North Indian Ocean: Insights from ENSO

D Das ^{1,5,*}, S Chiao ¹, C Roychoudhury ², F Khan ³, S Chaudhuri ³ and S Mukherjee ⁴

¹ NOAA Cooperative Science Center in Atmospheric Sciences and Meteorology, Howard University, Washington DC, USA

² Department of Hydrology and Atmospheric Sciences, University of Arizona, Tucson, AZ, USA

³ Department of Atmospheric Sciences, University of Calcutta, Kolkata, India

⁴ Department of Environmental Science, Amity University, Kolkata, India

⁵ COLA/George Mason University (GMU), Fairfax, VA

* Correspondence: debanjana.das@howard.edu

Abstract: Tropical cyclones (TC) are one of the deadliest natural meteorological hazards and the most frequent cause of natural disasters. The El-Niño Southern Oscillation (ENSO), a tropical ocean-atmosphere interaction, is known to significantly impact cyclonic systems over global ocean basins. This study investigates the variability of TC activity in presence of ENSO over the North Indian Ocean (NIO), comprising of the Arabian Sea (ARB) and the Bay of Bengal (BOB) basins during the pre- and post-monsoon season, using accumulated cyclone energy (ACE) over the last 26 years. Our analysis reveals a significant rise in cyclone intensity over the past two decades, with eight of the ten most active years occurring since the 2000s. Total ACE over the NIO is found to be higher in La-Niña. Higher ACE observed over ARB is strongly associated with a combination of elevated sea surface height (SSH) anomaly and low vertical wind shear during the El-Niño episodes, with higher sea surface temperatures (SST) during the post-monsoon season. Whereas in the BOB, El Niño not only reduces ACE but also decreases basin-wide variability, and more pronounced effect during the post-monsoon season, coinciding with warmer SST and higher SSH along the coast during La-Niña.

Keywords: tropical cyclone; ENSO; ACE; SST; SSH

1. Introduction

Tropical cyclones (TCs) are among the most devastating tropical weather phenomena with huge loss of lives and damage to property. Around 7% of global tropical cyclones occur in the north Indian Ocean (NIO). The number of cyclones occurring over Bay of Bengal (BOB) is greater than the Arabian Sea (ARB), approximately four times higher [1]. Identification of the trends in their frequency and intensity over the NIO are very important for the coastal regions as 5-6 tropical cyclones form over this basin every year on an average [2]. Generally, more TCs occur in the NIO in the post-monsoon season (primary TC peak season) and pre-monsoon season (secondary TC peak season). A few cyclones develop during monsoon months as well. The atmospheric and oceanic conditions and the variation in TC activity in the BOB have been studied extensively earlier [3–7]. A relationship between Madden-Julian Oscillation (MJO) and tropical cyclones over Indian Ocean and western Pacific has also been identified [8]. The El-Niño Southern Oscillations (ENSO) have significant impact on the cyclonic activity over different ocean basins [9–11]. During ENSO, sea surface temperatures (SST) has been observed to change over the tropical eastern Pacific which affects the atmospheric circulation in the equatorial Pacific and at the same time the Walker Circulation also changes which greatly influences the oceanic and atmospheric conditions globally [12,13]. The ENSO events have a substantial influence on TCs by modulating large-scale circulation [14–17]. Earlier studies have investigated the relationship between ENSO and seasonal TC activity in different tropical basins [18,19]. In a study the impact of ENSO and MJO on TC activity over the south Indian Ocean has been analyzed as well [20]. Trends in TC activity in relation to ENSO in the Southern hemisphere have also been investigated [21]. ENSO events also have significant impacts on the locations of the tropical

cyclogenesis and hurricane intensity [22–24]. In the Atlantic basin during the El-Niño (La-Niña) years, less (more) cyclones have been observed. The El-Niño phase of ENSO suppresses the formation of TCs in the north Atlantic basin. Intensity forecasts of tropical cyclones have been a major focus of the NIO region. *Chaudhuri et al. 2015* estimated the predictability of severe tropical cyclones over the NIO by observing features of cyclonic depression with a condition-decision support system of rough set theory [19]. Artificial Neural Networks have also been developed for medium-range forecasts of cyclogenesis [25]. Comparatively, less research has been conducted over the NIO in relation to ENSO and TC activity. Past research shows a decline in TC activity over BOB in the months of May and November during the warm phases of ENSO and it was observed that the TC frequency in the NIO has a prominent ENSO cycle (2–5 years) during May–November. *Albert et al. 2022* has shown that TCs are relatively more pronounced over the BOB during La-Niña and negative IOD (Indian Ocean Dipole) years [10,26,27]. TC activity has been studied using different metrics which includes annual storm counts, hurricane categories, power dissipation index (PDI) and the accumulated cyclone energy (ACE) index [28–30]. The ACE metric is similar to the PDI and includes intensity and duration information for each individual TC [31]. Some research indicates that changes in PDI correlate with increased sea surface temperatures (SST) in the Atlantic [3,32]. While some studies have suggested a decline in ACE, others have reported an increase, particularly in the context of global warming scenarios [6,31,33,34].

The purpose of this study is to investigate the connection between the El Niño Southern Oscillation (ENSO) signals to TC activity in the basins of NIO and identify the possible oceanic and atmospheric processes that modulate them using the ACE index. By conducting separate analyses for the ARB and BOB regions, we aim to enhance our understanding of TC variability in this complex, climate-sensitive zone.

This research paper has four sections. In Section 2, we describe the datasets and the methods used. Section 3 discusses the main findings, including the statistics of TC activity and ACE and provides an analysis of the impacts of ENSO on TCs. In Section 4, we discuss the implications and the summarize our findings.

2. Data and Methods

2.1. Data

Different types of satellites and ocean analysis products have been used in this study. The best track data for cyclonic disturbances over the north Indian Ocean, generated by the Regional Specialised Meteorological Centre (RSMC), IMD, India <http://www.rsmcnewdelhi.imd.gov.in/index.php> are used. The period of study is 1990 -2018. The daily sea surface temperature (SST) is used from NOAA [35]. GODAS Sea Surface Height (SSH) data is also used from NOAA.

2.2. Methodology

The cyclonic systems have been classified with respect to wind speed according to IMD (India Meteorological Department) criteria as follows; Depression (D) (17–27 kt), Deep Depression (DD) (28–33 kt), Cyclonic Storm (CS) (34–47 kt), Severe Cyclonic Storm (SCS) (48–63 kt), Very Severe Cyclonic Storm (VSCS) (64–119 kt) and Super Cyclonic Storm (SUCS) (>120 kt). In this study, the focus is only on the TCs of CS and higher categories. The definition of El-Niño and La-Niña events are based on the analysis of the Oceanic Niño Index (ONI) according to world meteorological organization (WMO). The El-Niño years are defined when ONI is above 0.5°C for a minimum of 5 consecutive months and the La-Niña years are defined when ONI is below - 0.5 °C for minimum of 5 consecutive months according to WMO. The same criterion has been used in this study to categorize El-Niño and La-Niña years. The present investigation focuses on the variability of ACE index with respect to El-Niño and La-Niña during the pre-(March-May) and post- monsoon (Oct-Dec) season in order to understand the TC activity over NIO and its link with the El-Niño and La-Niña events. Values of ACE for the pre- and post-monsoon season are obtained by computing the sum of the

squares of the estimated 6 hourly maximum sustained wind speed (kt^2) over the lifetime of a TC as it reaches to CS and higher category and subsequently adding them for all TCs over the entire season under consideration. The annual ACE values are also computed by summing the values of ACE for all the TCs occurring in a year. The unit of ACE is $10^4 kt^2$, and for use as an index the unit is assumed. The values of ACE used in the present study are computed as:

$$ACE = 10^4 \sum v_{\max}^2 \quad (1)$$

where v_{\max} is estimated sustained wind speed of the system in knots.

3. Results

3.1. ACE Variability Across the North Indian Ocean, Arabian Sea, and Bay of Bengal Basins

The duration of different categories of cyclonic systems forming over BOB and ARB has been estimated for both pre-monsoon and post monsoon season during El-Niño and La-Niña years (Table 1). It is observed that during the pre-monsoon season the duration of the CS category of cyclones is maximum over BOB and ARB in the El-Niño years. However, in the La-Niña years the duration of D category of cyclones is more over BOB followed by the CS categories while the duration of ESCS category is more over ARB.

Table 1. Duration in Hours for Cyclonic Systems Occurring During Pre-Monsoon and Post-Monsoon Seasons in El Niño and La-Niña Years (1990-2018) over BOB and ARB.

Season	ENSO	Basin	D	DD	CS	SCS	VSCS	ESCS	SUCS
Pre-Monsoon	El Niño	ARB	78	54	216	66	0	0	0
		BOB	138	108	330	102	90	102	24
	La-Niña	ARB	60	108	90	12	48	102	0
		BOB	282	132	162	84	0	0	0
Post-Monsoon	El Niño	ARB	258	252	384	186	120	210	0
		BOB	564	264	570	30	0	0	0
	La-Niña	ARB	528	564	174	60	0	0	0
		BOB	570	462	456	234	288	216	0

The observation suggests that either the occurrence of CS categories of cyclones have increased, or the lifetime of such cyclones has become more over BOB. Conversely, during the post-monsoon season the duration of CS category of cyclones is observed to be more in the El-Niño years and the duration of DD category of cyclones is more in the La-Niña years. It is observed that during the pre-monsoon season in the El-Niño years the cyclones of higher categories than CS are more over BOB. However, during the post-monsoon season in the El-Niño years the maximum cyclones over BOB are of CS category whereas cyclones of CS and higher categories are more over ARB. Likewise, the number of cyclones occurring in the La-Niña years during pre- and post-monsoon season is estimated (Table 2). It is observed that the cyclones of CS category are more and just one case of SCS category prevails during the pre-monsoon season over BOB while one case each of CS and ESCS categories is observed over ARB. During the post-monsoon season the cyclones of CS and higher categories are more over BOB in the La-Niña years.

Table 2. Number of TC Cases During Pre-Monsoon and Post-Monsoon Seasons in El Niño and La-Niña Years (1990-2018) over BOB and ARB.

Season	ENSO	Basin	CS	SCS	VSCS	ESCS	SUCS	Total
Pre-Monsoon	El Nino	ARB	1	1	0	0	0	2
		BOB	1	1	0	3	0	5
	La-Niña	ARB	1	0	0	1	0	2
		BOB	2	2	0	0	0	4
Post-Monsoon	El Nino	ARB	2	3	2	4	0	11
		BOB	7	0	0	0	0	7
	La-Niña	ARB	1	0	0	1	0	2
		BOB	2	2	0	0	0	4

The total ACE values during El-Niño and La-Niña years are estimated (Figure 1). It is observed that during the El-Niño years the ACE of ARB and BOB is comparable while for La-Niña years BOB has higher ACE than ARB. Nevertheless, during El-Niño the ACE values of the BOB basins and NIO is less than the La-Niña years. The result further shows that the ACE increases during the cold regime, emphasizing the correlation between ENSO and TC activity in the NIO.

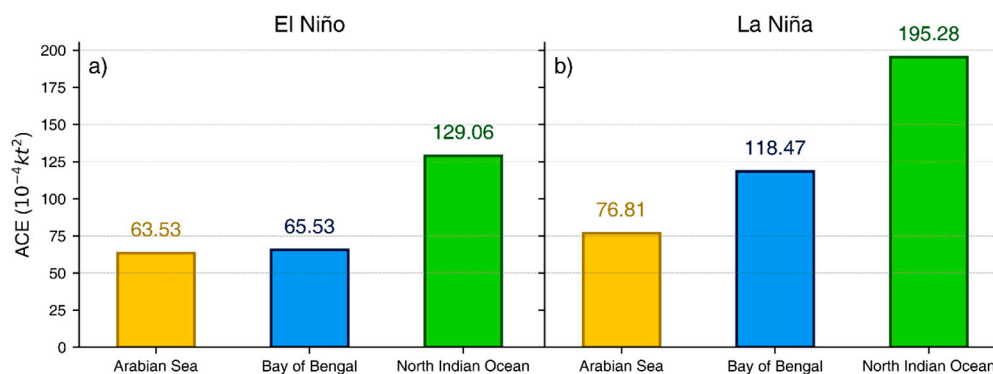


Figure 1. Total ACE values for (a) El-Niño and (b) La-Niña years over the ARB Sea, BOB and North Indian Ocean.

During El Niño, ACE is 129.06×10^4 knots², while in La-Niña, it jumps to 195.28×10^4 knots². Notably, the ACE increase is more pronounced over the Bay of Bengal than the Arabian Sea during the transition from El Niño to La-Niña. This distinctive ACE fluctuation is profoundly shaped by the unique physio-chemical attributes intrinsic to each ocean basin. This, in turn, affects ACE through changes in the strength of winds.

Figure 2 illustrates the average ACE values for the pre-monsoon and post-monsoon seasons during El-Niño and La-Niña phases. The data covers the years 1990-2015 and is segmented for both for the Bay of Bengal (BOB) and Arabian Sea (ARB). This depiction provides a comprehensive view of how ACE behaves in response to El-Niño and La-Niña events across these specific regions during different seasons. The blue bars represent La-Niña, and the red bars represent El-Niño. Notably, the average maximum ACE is higher (15.88) over the Arabian Sea during El-Niño, specifically during post-monsoon months. Conversely, over the Bay of Bengal, the maximum ACE is observed during La-Niña's post-monsoon phase. Figure 2 effectively showcases how El Niño and La-Niña events not only impact the North Indian Ocean but also exhibit detectable differences in their basin-wide effects. These climatic phases influence seasonal ACE variations distinctively, not only across ocean basins but also within them. Remarkably, the basin-wide cyclonic energy pattern undergoes a reversal during El-Niño and La-Niña phases, emphasizing their complex influence.

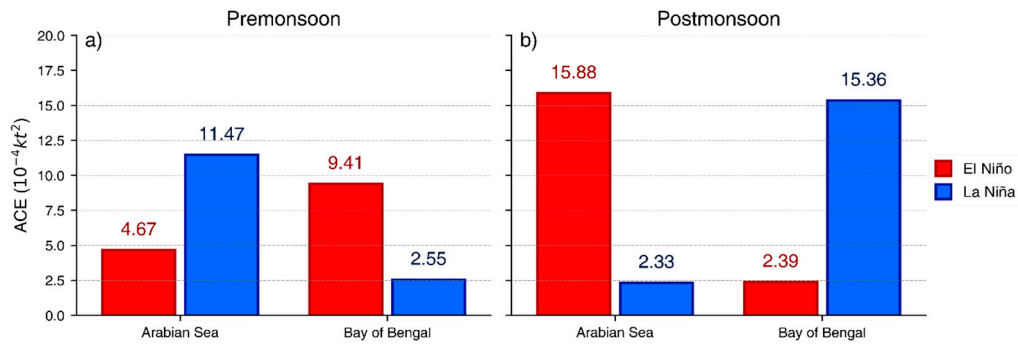


Figure 2. Average ACE values for the pre-monsoon and post-monsoon season during El-Niño and La-Niña phase respectively during the period 1990-2018.

A comprehensive box-whisker plot of Accumulated Cyclone Energy (ACE) for all years is presented (Figure 3), specifically differentiating between El-Niño and La-Niña years. The analysis focuses on post-monsoon, monsoon, pre-monsoon, and annual periods across the Arabian Sea (ARB), Bay of Bengal (BOB), and the entire North Indian Ocean (NIO) region. Figure 3 employs a color scheme where blue designates the Arabian Sea, orange corresponds to the North Indian Ocean, and green is utilized for the Bay of Bengal. Importantly, we observe that the average and range of ACE values tend to be higher across all years, compared to only El-Niño years. Conversely, during La-Niña years, ACE's variability and average are notably higher across all years, and this distinction is more pronounced during both El-Niño and La-Niña occurrences.

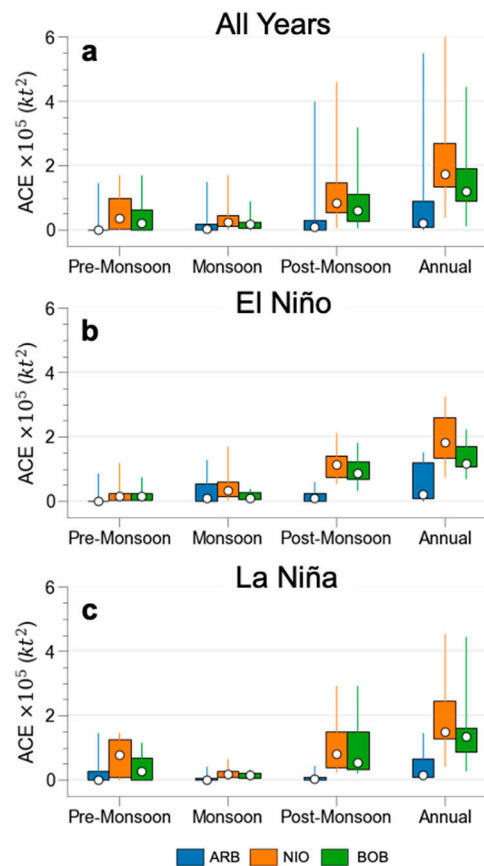


Figure 3. Box-Whisker Plots Over 1982-2020: Post-Monsoon, Monsoon, Pre-Monsoon, and Annual Analysis of Accumulated Cyclone Energy (ACE) Across Arabian Sea, Bay of Bengal, and North Indian Ocean for all years (a), El-Niño (b) and La-Niña (c) years.

The ACE index for the Arabian Sea (ARB) and the Bay of Bengal (BOB) from 1990 to 2018 indicates an increasing trend in both basins, with a more pronounced increase observed in the ARB. ACE values in the BOB exhibit less variability, while the ARB shows significant fluctuations, with some years experiencing notably higher or negligible ACE values. Moreover, ACE values in the BOB are consistently higher than those in the ARB (Figure. 4).

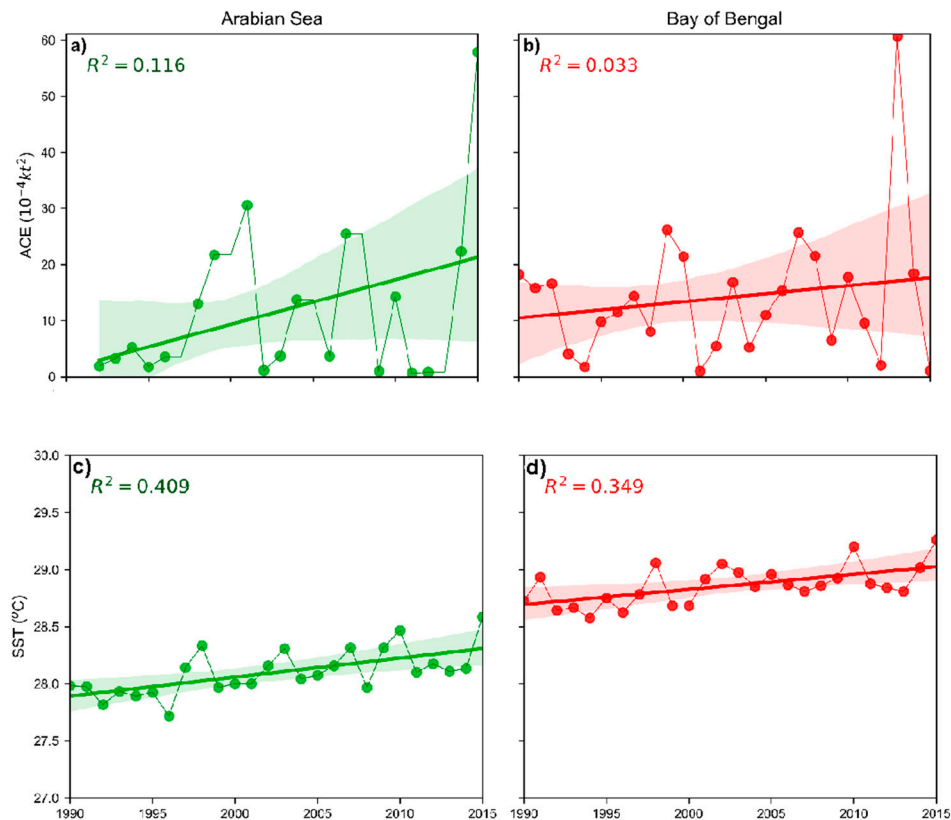


Figure 4. ACE and SST over ARB and BOB from 1990 – 2015.

Regarding sea surface temperature (SST), both the ARB and BOB show rising trends over the study period, aligning with global tropical cyclone trends associated with increasing temperatures. The ARB experiences a more substantial SST increase compared to the BOB. The observed R² values for SST trends are 0.409 (ARB) and 0.349 (BOB) (Figure 4).

3.2. Spatio-Temporal Variability of Atmospheric and Oceanic Modulation During ENSO Phases

SST is an important parameter which plays an important role in the development of tropical cyclones. The SST anomaly during the post monsoon and pre-monsoon season of El-Niño and La-Niña years is depicted (Figure 7). In panels corresponding to El-Niño conditions, SST anomalies are observed to exhibit distinctive patterns during both the post-monsoon and pre-monsoon seasons. In panels (b) and (d), representing La-Niña phases, the SST anomalies portray contrasting characteristics in the two respective seasons. These variations highlight the pronounced influence of El-Niño and La-Niña events on regional sea surface temperature dynamics, accentuated across different temporal segments.

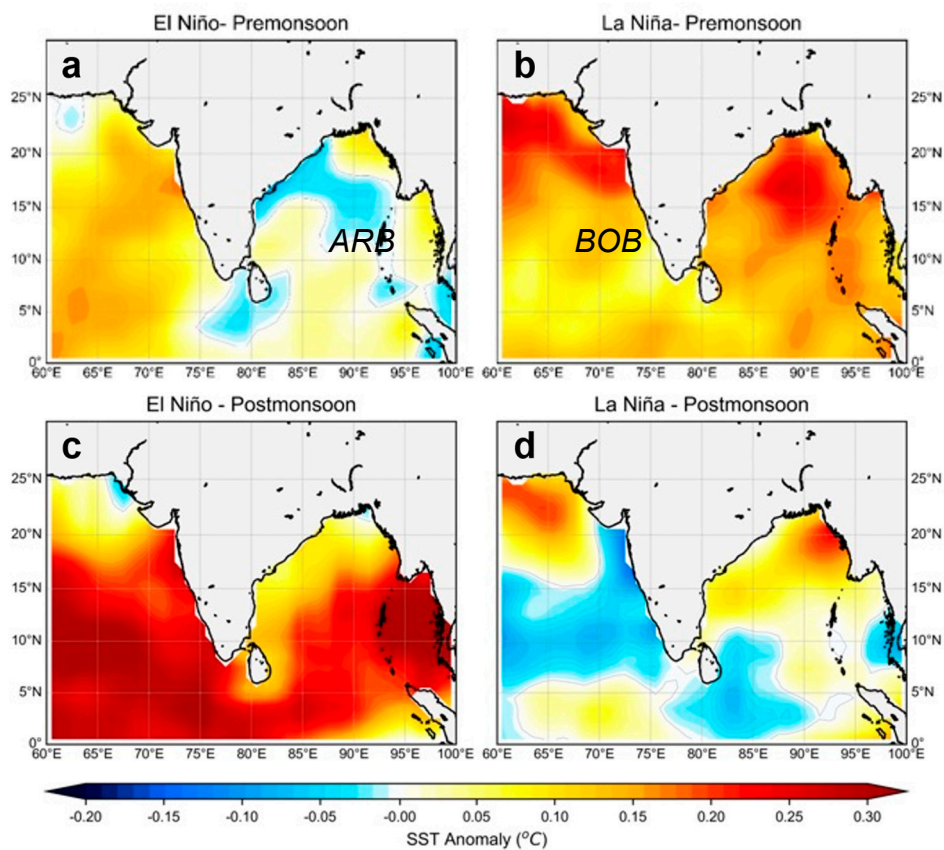


Figure 5. Sea Surface Temperature (SST) anomaly for (a, c) El-Niño and (b, d) La-Niña phase during (a, b) post-monsoon season and (c, d) pre-monsoon season.

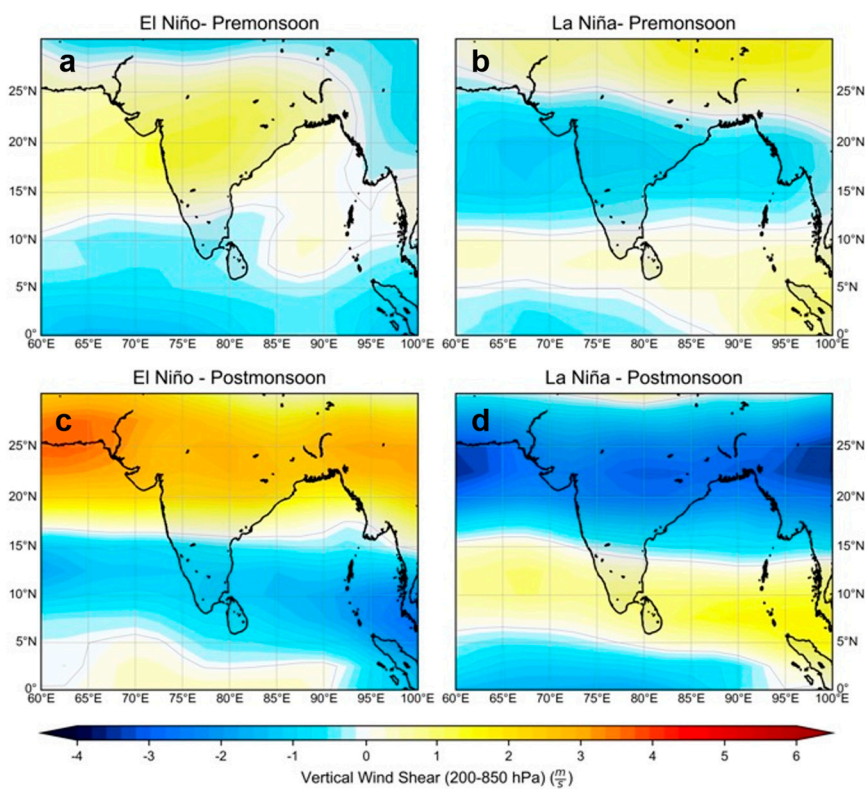


Figure 6. Vertical wind shear between 200hPa and 850 hPa for the (a) post-monsoon season and (b) pre-monsoon during El-Niño, normal, and La-Niña events.

For the post monsoon season during El-Niño years the SST shows positive anomaly for both ARB and BOB with higher values over the ARB. For the La-Niña years negative anomaly is observed for both ARB and BOB. The positive anomalies in SST over ARB and BOB in post monsoon season is observed to be directly correlated with El-Niño which aids in warming the water of the ocean. For the pre-monsoon season, the BOB has negative and greater SST anomaly while ARB has less SST anomaly during El-Niño years. During La-Niña years ARB has positive SST anomaly and positive anomaly is observed in the upper BOB and negative SST anomaly is observed in the lower regions of BOB, however, ARB has higher positive anomaly. From the above results it can be inferred that the effect of ENSO is greater during post-monsoon season as the peak of ENSO phenomena occurs around November-January [36]. Furthermore, the effect of ENSO during post-monsoon and pre-monsoon seasons is contradictory.

Weak vertical shear of horizontal wind between lower (850 hPa) and upper troposphere (200 hPa) also assists in the formation of cyclones [7]. The average vertical wind shear for post-monsoon and pre-monsoon seasons during El-Niño, neutral and La-Niña years has been estimated (Figure 6). It is evident that the wind shear over both ARB and BOB is low and almost same in both El-Niño and La-Niña years for the pre monsoon period as it is in the normal case, and it is lowest in southern portions of ARB. The wind shear for post monsoon season in the La-Niña years is slightly greater in the BOB than ARB whereas for El-Niño years and normal years the wind shear is low and similar in BOB and ARB. Figure 7 displays Sea Surface Height (SSH) anomalies distinctly portray divergent oceanic characteristics corresponding to these phases. Significantly, the magnitudes exhibit substantial variability across the two seasons. Notably, the anomalies exhibit a strengthening trend during La-Niña's pre-monsoon to post-monsoon transition. Furthermore, the SSH gradient between the Arabian Sea and the Bay of Bengal becomes pronounced.

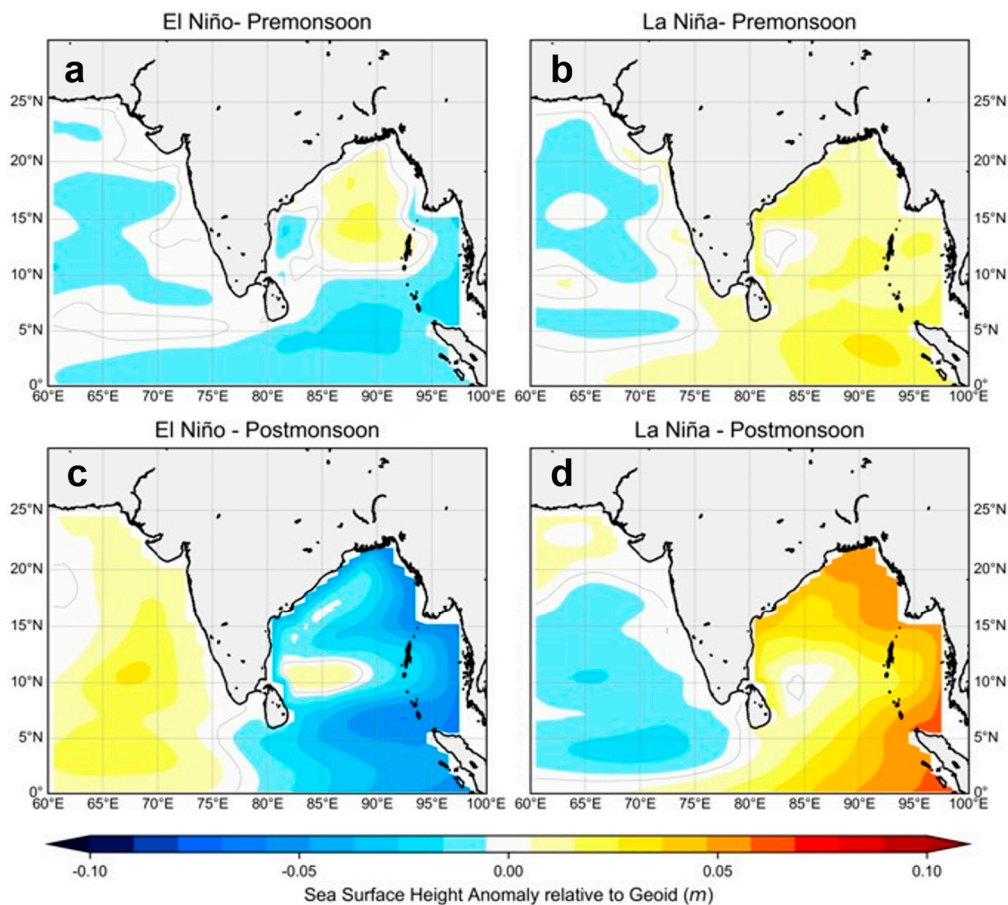


Figure 7. Sea Surface Height (SSH) anomaly for (a, c) El-Niño and (b, d) La-Niña phase during (a, b) post-monsoon season and (c, d) pre-monsoon season.

4. Conclusions

ENSO and its relation to TC activity in the ARB and BOB during the pre-monsoon and post-monsoon season are studied for the period of 1990-2018. This study shows that ENSO significantly and differently affects the tropical cyclone activity over BOB and ARB during the El-Niño and La-Niña years. During La-Niña (El-Niño) phases, the TC activity is observed to be relatively more (less) pronounced in the NIO. The ACE values for El-Niño years for ARB and BOB do not show any significant difference and for La-Niña years ACE is greater for BOB than ARB. ACE in the La-Niña phase. Higher SST is observed in the post-monsoon season which along with high SSH and low wind shear leads to higher ACE values in ARB during El-Niño years. In the La-Niña phase ACE is more in BOB in post monsoon season but SST is not higher in BOB. So, SST may not be a factor for higher ACE values in BOB. SSH is greater in the post-monsoon season in BOB which along with low wind shear may be responsible for greater ACE values in BOB. The result shows that during the post-monsoon season tropical cyclone activity measured in terms of ACE is more over ARB during El-Niño phase while ACE is more over BOB during the La-Niña phase.

During La-Niña, sea surface temperatures in the central and eastern equatorial Pacific Ocean are cooler than average. However, the impact of La-Niña on tropical cyclone activity is more complex than simply cooler waters. Here's why La-Niña can lead to higher Accumulated Cyclone Energy (ACE) over the North Indian Ocean. La-Niña is associated with changes in atmospheric circulation patterns. These shifts can lead to favorable conditions for tropical cyclone development in certain regions, including the North Indian Ocean. While La-Niña brings cooler waters to the equatorial Pacific, it can lead to warmer-than-average sea surface temperatures in other areas, such as the western Indian Ocean, which can support cyclone formation. La-Niña tends to reduce wind shear in the North Indian Ocean. Wind shear, which is the change in wind speed and direction with altitude, can inhibit cyclone development. When wind shear is low, it allows cyclones to form and intensify more easily, contributing to higher ACE values. La-Niña can enhance atmospheric instability, which is a key factor for cyclone development. The presence of unstable air encourages the rising motion necessary for cyclone formation. This increased instability can lead to more frequent and stronger cyclones during La-Niña. La-Niña or El-Niño doesn't act in isolation; it interacts with other climate patterns such as the Indian Ocean Dipole (IOD). A positive IOD phase, which often coincides with La-Niña, can lead to warmer waters in the western Indian Ocean, further supporting cyclone development. While La-Niña does bring cooler waters to some regions, its impact on cyclone activity is influenced by a combination of factors including atmospheric circulation changes, wind shear, atmospheric instability, and interactions with other climate patterns. These factors can create conditions conducive to increased cyclone activity and higher ACE values in the North Indian Ocean despite the cooling effect of La-Niña in the Pacific.

Given the distinct behavior of cyclonic activity in different ocean basins, treating them separately rather than using a larger geographical domain like the North Indian Ocean can indeed lead to better predictability of tropical cyclone activity. In summary, a basin-specific approach, rather than a broader geographical domain, can enhance the precision and reliability of tropical cyclone predictions, ultimately contributing to better preparedness and response strategies for vulnerable regions.

Author Contributions: Conceptualization, D. Das, S Chaudhuri; Methodology, D. Das, F. Khan, C. Roychoudhury; Analysis, D. Das, F. Khan, C. Roychoudhury; Data Curation, F. Khan, D. Das, S. Chaudhuri; Writing—Original Draft, D. Das; Writing—Review and Editing, D. Das, F. Khan, S. Chiao, C. Roychoudhury, S. Mukherjee; Funding Acquisition, S. Chiao, S Chaudhuri, D Das.

Funding: This research was partially supported by NASA (grant NNX14AM19G). The 2nd author is supported by the U.S. Department of Commerce, National Oceanic and Atmospheric Administration, Educational Partnership Program under Agreement No. NA22SEC4810015.

Data Availability Statement: The data presented in this study are openly available via the links provided in the data section. More detailed information can be obtained upon request to the corresponding authors.

Conflicts of Interest: The authors declare no conflict of interest.

References

1. Lin, I.-I.; Chen, C.-H.; Pun, I.-F.; Liu, W.T.; Wu, C.-C. Warm Ocean Anomaly, Air Sea Fluxes, and the Rapid Intensification of Tropical Cyclone Nargis (2008). *Geophysical Research Letters* **2009**, *36*. <https://doi.org/10.1029/2008GL035815>.
2. Tiwari, G.; Kumar, P.; Javed, A.; Mishra, A.K.; Routray, A. Assessing Tropical Cyclones Characteristics over the Arabian Sea and Bay of Bengal in the Recent Decades. *Meteorol Atmos Phys* **2022**, *134*, 44. <https://doi.org/10.1007/s00703-022-00883-9>.
3. Vecchi, G.A.; Soden, B.J. Effect of Remote Sea Surface Temperature Change on Tropical Cyclone Potential Intensity. *Nature* **2007**, *450*, 1066–1070. <https://doi.org/10.1038/nature06423>.
4. Simpson, R.H. The Hurricane Disaster—Potential Scale. *Weatherwise* **1974**, *27*, 169–186. <https://doi.org/10.1080/00431672.1974.9931702>.
5. Thiébaux, J.; Rogers, E.; Wang, W.; Katz, B. A New High-Resolution Blended Real-Time Global Sea Surface Temperature Analysis. *Bulletin of the American Meteorological Society* **2003**, *84*, 645–656. <https://doi.org/10.1175/BAMS-84-5-645>.
6. Klotzbach, P.J. Trends in Global Tropical Cyclone Activity over the Past Twenty Years (1986–2005). *Geophysical Research Letters* **2006**, *33*. <https://doi.org/10.1029/2006GL025881>.
7. Gray, M.. W. Hurricanes: Their Formation, Structure and Likely Role in the General Circulation. *Meteorology over the Tropical Oceans* **1979**, 155–218.
8. Lakshani, W.A.E.; Zhou, W. Observed Decadal Shifts and Trends in Global Tropical Cyclone Activities from 1980 to 2021. *Atmospheric and Oceanic Science Letters* **2023**, *16*, 100321. <https://doi.org/10.1016/j.aosl.2022.100321>.
9. Gray, W.M. Tropical Cyclone Genesis. phd, Colorado State University. Libraries, 1975.
10. Ho, C.-H.; Kim, J.-H.; Jeong, J.-H.; Kim, H.-S.; Chen, D. Variation of Tropical Cyclone Activity in the South Indian Ocean: El Niño–Southern Oscillation and Madden-Julian Oscillation Effects. *Journal of Geophysical Research: Atmospheres* **2006**, *111*. <https://doi.org/10.1029/2006JD007289>.
11. Chia, H.H.; Ropelewski, C.F. The Interannual Variability in the Genesis Location of Tropical Cyclones in the Northwest Pacific. *Journal of Climate* **2002**, *15*, 2934–2944. [https://doi.org/10.1175/1520-0442\(2002\)015<2934:TIVITG>2.0.CO;2](https://doi.org/10.1175/1520-0442(2002)015<2934:TIVITG>2.0.CO;2).
12. Goswami, B.N.; Ajayamohan, R.S.; Xavier, P.K.; Sengupta, D. Clustering of Synoptic Activity by Indian Summer Monsoon Intraseasonal Oscillations. *Geophysical Research Letters* **2003**, *30*. <https://doi.org/10.1029/2002GL016734>.
13. Goldenberg, S.B.; Shapiro, L.J. Physical Mechanisms for the Association of El Niño and West African Rainfall with Atlantic Major Hurricane Activity. *Oceanographic Literature Review* **1997**, *4*, 307.
14. Goldenberg, S.B.; Shapiro, L.J. Physical Mechanisms for the Association of El Niño and West African Rainfall with Atlantic Major Hurricane Activity. *Journal of Climate* **1996**, *9*, 1169–1187. [https://doi.org/10.1175/1520-0442\(1996\)009<1169:PMFTAO>2.0.CO;2](https://doi.org/10.1175/1520-0442(1996)009<1169:PMFTAO>2.0.CO;2).
15. Villarini, G.; Vecchi, G.A. North Atlantic Power Dissipation Index (PDI) and Accumulated Cyclone Energy (ACE): Statistical Modeling and Sensitivity to Sea Surface Temperature Changes. *Journal of Climate* **2012**, *25*, 625–637. <https://doi.org/10.1175/JCLI-D-11-00146.1>.
16. Wang, B.; Chan, J.C.L. How Strong ENSO Events Affect Tropical Storm Activity over the Western North Pacific. *Journal of Climate* **2002**, *15*, 1643–1658. [https://doi.org/10.1175/1520-0442\(2002\)015<1643:HSEEAT>2.0.CO;2](https://doi.org/10.1175/1520-0442(2002)015<1643:HSEEAT>2.0.CO;2).
17. Franzke, C.L.E.; Torelló i Sentelles, H. Risk of Extreme High Fatalities Due to Weather and Climate Hazards and Its Connection to Large-Scale Climate Variability. *Climatic Change* **2020**, *162*, 507–525. <https://doi.org/10.1007/s10584-020-02825-z>.
18. Chaudhuri, S.; Basu, D.; Das, D.; Goswami, S.; Varshney, S. Swarm Intelligence and Neural Nets in Forecasting the Maximum Sustained Wind Speed along the Track of Tropical Cyclones over Bay of Bengal. *Nat Hazards* **2017**, *87*, 1413–1433. <https://doi.org/10.1007/s11069-017-2824-4>.
19. Chaudhuri, S.; Dutta, D.; Goswami, S.; Middey, A. Track and Intensity Forecast of Tropical Cyclones over the North Indian Ocean with Multilayer Feed Forward Neural Nets. *Meteorological Applications* **2015**, *22*, 563–575. <https://doi.org/10.1002/met.1488>.
20. Ho, C.-H.; Kim, J.-H.; Jeong, J.-H.; Kim, H.-S.; Chen, D. Variation of Tropical Cyclone Activity in the South Indian Ocean: El Niño–Southern Oscillation and Madden-Julian Oscillation Effects. *Journal of Geophysical Research: Atmospheres* **2006**, *111*. <https://doi.org/10.1029/2006JD007289>.
21. Ogata, T. Seasonality of Relationship between Tropical Cyclone Frequency over the Southern Hemisphere and Tropical Climate Modes. *Atmosphere* **2023**, *14*, 546. <https://doi.org/10.3390/atmos14030546>.
22. Ke, M.; Wang, Z.; Pan, W.; Luo, H.; Yang, S.; Guo, R. Extremely Strong Western Pacific Subtropical High in May 2021 Following a La Niña Event: Role of the Persistent Convective Forcing over the Indian Ocean. *Asia-Pac J Atmos Sci* **2023**, *59*, 47–58. <https://doi.org/10.1007/s13143-022-00300-6>.
23. Landsea, C.W.; Pielke, R.A.; Mestas-Nuñez, A.M.; Knaff, J.A. Atlantic Basin Hurricanes: Indices of Climatic Changes. *Climatic Change* **1999**, *42*, 89–129. <https://doi.org/10.1023/A:1005416332322>.

24. Lin, I.-I.; Camargo, S.J.; Patricola, C.M.; Boucharel, J.; Chand, S.; Klotzbach, P.; Chan, J.C.L.; Wang, B.; Chang, P.; Li, T.; et al. ENSO and Tropical Cyclones. In *El Niño Southern Oscillation in a Changing Climate*; American Geophysical Union (AGU), 2020; pp. 377–408 ISBN 978-1-119-54816-4.
25. Kikuchi, K.; Wang, B.; Fudeyasu, H. Genesis of Tropical Cyclone Nargis Revealed by Multiple Satellite Observations. *Geophysical Research Letters* **2009**, *36*. <https://doi.org/10.1029/2009GL037296>.
26. Albert, J.; Krishnan, A.; Bhaskaran, P.K.; Singh, K.S. Role and Influence of Key Atmospheric Parameters in Large-Scale Environmental Flow Associated with Tropical Cyclogenesis and ENSO in the North Indian Ocean Basin. *Clim Dyn* **2022**, *58*, 17–34. <https://doi.org/10.1007/s00382-021-05885-8>.
27. Gray, W.M. Atlantic Seasonal Hurricane Frequency. Part I: El Niño and 30 Mb Quasi-Biennial Oscillation Influences. *Monthly Weather Review* **1984**, *112*, 1649–1668. [https://doi.org/10.1175/1520-0493\(1984\)112<1649:ASHFPI>2.0.CO;2](https://doi.org/10.1175/1520-0493(1984)112<1649:ASHFPI>2.0.CO;2).
28. Webster, P.J.; Holland, G.J.; Curry, J.A.; Chang, H.-R. Changes in Tropical Cyclone Number, Duration, and Intensity in a Warming Environment. *Science* **2005**, *309*, 1844–1846. <https://doi.org/10.1126/science.1116448>.
29. Waple, A.M.; Lawrimore, J.H.; Halpert, M.S.; Bell, G.D.; Higgins, W.; Lyon, B.; Menne, M.J.; Gleason, K.L.; Schnell, R.C.; Christy, J.R.; et al. Climate Assessment for 2001. *Bulletin of the American Meteorological Society* **2002**, *83*, S1–S62.
30. Bell, G.; Halpert, M.; Schnell, R.; Higgins, R.; Lawrimore, J.; Kousky, V.; Tinker, R.; Thiaw, W.; Chelliah, M.; Artusa, A. The 1999 North Atlantic and Eastern North Pacific Hurricane Seasons [in “Climate Assessment for 1999”]. *Bulletin of the American Meteorological Society* **2000**, *81*, S19–S22.
31. Maue, R.N. Recent Historically Low Global Tropical Cyclone Activity. *Geophysical Research Letters* **2011**, *38*. <https://doi.org/10.1029/2011GL047711>.
32. Bamston, A.G.; Chelliah, M.; Goldenberg, S.B. Documentation of a Highly ENSO-related Sst Region in the Equatorial Pacific: Research Note. *Atmosphere-Ocean* **1997**, *35*, 367–383. <https://doi.org/10.1080/07055900.1997.9649597>.
33. Fahad, A.A.; Reale, O.; Molod, A.; Sany, T.A.; Ahammad, M.T.; Menemenlis, D. The Role of Tropical Easterly Jet on the Bay of Bengal’s Tropical Cyclones: Observed Climatology and Future Projection. *Journal of Climate* **2023**, *36*, 5825–5840. <https://doi.org/10.1175/JCLI-D-22-0804.1>.
34. Klotzbach, P.J.; Wood, K.M.; Schreck III, C.J.; Bowen, S.G.; Patricola, C.M.; Bell, M.M. Trends in Global Tropical Cyclone Activity: 1990–2021. *Geophysical Research Letters* **2022**, *49*, e2021GL095774. <https://doi.org/10.1029/2021GL095774>.
35. Reynolds, R.W.; Smith, T.M.; Liu, C.; Chelton, D.B.; Casey, K.S.; Schlax, M.G. Daily High-Resolution-Blended Analyses for Sea Surface Temperature. *Journal of Climate* **2007**, *20*, 5473–5496. <https://doi.org/10.1175/2007JCLI1824.1>.
36. Tziperman, E.; Cane, M.A.; Zebiak, S.E.; Xue, Y.; Blumenthal, B. Locking of El Niño’s Peak Time to the End of the Calendar Year in the Delayed Oscillator Picture of ENSO. *Journal of climate* **1998**, *11*, 2191–2199.

Disclaimer/Publisher’s Note: The statements, opinions and data contained in all publications are solely those of the individual author(s) and contributor(s) and not of MDPI and/or the editor(s). MDPI and/or the editor(s) disclaim responsibility for any injury to people or property resulting from any ideas, methods, instructions or products referred to in the content.